EUROPEAN ORGANIZATION FOR NUCLEAR RESEARCH

PH III-67/42
25 September 1967

PHYSICS III COMMITTEE

PROPOSAL FOR CONTINUATION AND FURTHER WORK ON $(\pi^+,2p)$ AND (π^+,π^+p) REACTIONS

by

T. Bressani, G. Charpak, J. Favier, L. Massonnet, and Č. Zupančič

(received 25 September 1967)

***

Our group has completed the measurements on the $(\pi^+,2p)$ reaction in several nuclei, mainly at an incident energy of 80 MeV. The measurements have been partially analysed and some preliminary results are presented in the attached report. Lately, the experiment has been extended to incident energies of 150, 200, and 260 MeV. In general, no surprising results were obtained. However, at 260 MeV the excitation-energy spectrum of residual (pn) pairs from the $(\pi^+,2p)$ reaction in ^{4}He shows indications of rather narrow peaks in the region between 30 MeV and 100 MeV. Their statistical significance is not very great since we only ran the experiment for about 6 hours. If confirmed, they may still be due to some instrumental effect which we do not yet understand. However, if these peaks were real, the consequences would be far-reaching and we feel that one should devote a few additional shifts to their investigation.

In the course of our measurements we observed that pions could be detected very well and could be distinguished from protons. Our range-measuring chambers may be used for the measurement of pion energies up to about 120 MeV, in spite of the large losses ($\sim$ 70% at 120 MeV) due to nuclear interactions.

We are thus in a position to study the quasi-free knock-out reactions (π^+,π^+p) in nuclei. The reasons that this is possible with pion intensities of the order of 10^4/sec are our large solid angle of acceptance and our ability to reconstruct the vertex inside a thick target. We expect to have counting rates of the order of 1000 good events per shift and a resolution in the excitation spectrum of better than 10 MeV. We feel that it should be worth while to make an exploratory study of this reaction in a few nuclei before our equipment is dismantled. The object of this study should be to establish a comparison with well-studied cases of (p,2p) reactions. Since pions of the available energies are much more strongly absorbed in nuclei than the protons which were used in (p,2p) reactions, such a comparison should provide a good test of the distorted-wave calculations of the knock-out reaction.

We propose that:

1) 10 shifts should be allocated for the study of the reaction $(\pi^+,2p)$ in ^{4}He at 260 MeV.

2) 20 shifts should be allocated for the study of (π^+,π^+p) reactions with the targets ^{6}Li, ^{7}Li, ^{12}C, $H_2{}^{16}O$ and $D_2{}^{16}O$. We should probably run at 260 MeV with the proton detected in the forward direction and the pion in the backward direction.

This work would be performed with our present equipment in the present location in the proton room. We should like to have the 30 shifts in December 1967 and January 1968.

THE $(\pi^+,2p)$ REACTIONS ON NUCLEI

by

T. Bressani, G. Charpak, J. Favier, L. Massonnet*),
W.E. Meyerhof**) and Č. Zupančič

1. INTRODUCTION

When a slow pion is absorbed in a nucleus by a single nucleon which takes all the available energy, the conservation of energy and momentum requires the nucleon to have a large momentum inside the nucleus before the absorption process. For a pion at rest this momentum would be 500 MeV/c, and it is known that not many nucleons have such high momenta. In the case of an absorption by a pair of nucleons, on the other hand, energy and momenta are easily balanced, the two nucleons going in opposite directions with a high relative momentum and a small momentum of their centre of mass. The fact that the absorption by a pair of nucleons is favoured makes pion absorption an ideal tool for the study of residual states with two holes in the internal shells.

In the impulse approximation, the nucleons not participating in the reaction are just spectators, and their momentum in the laboratory is the momentum they had relative to the pair of nucleons absorbing the pion, at the instant of the absorption. If well separated final excited states can be obtained from the $(\pi^+,2p)$ reactions, a study of the momentum distribution in the laboratory of these nuclei gives the distribution of momentum of these configurations relative to the pair of absorbing nucleons.

---

*) Present address: Institut de Physique Nucléaire, Orsay, France.
**) U.S. National Science Foundation Senior Postdoctoral Fellow, on leave from Stanford University, California, USA, 1966-7.

The choice of the geometry of detection can strongly influence the region of momentum distributions contributing to the reaction. We shall discuss this point when we come to the results obtained with ^{6}Li. Not very much theoretical work has been done since the first papers underlining the general interest of these reactions[1,7] and only the very recent work of Kopaleishvili[4,5] enters into the detailed structure of some specific nuclei. We shall summarize their results when discussing the results obtained for ^{12}C, ^{14}N and ^{16}O. In this report we wish to give a review of the results, and to show how necessary it is to have more theoretical investigations of this field.

2. EXPERIMENTAL TECHNIQUES

The 80-MeV π^{+} beam from the CERN Synchro-Cyclotron is impinging on a target T (Fig. 1). The beam is bent through 75° by the magnet MC, and two spark chambers (SP1 and SP2) at the exit of MC determine the direction and the position of the pions. Since the input direction of the pion beam, as determined by the collimation through the beam-transport system, is uncertain at most by ± 0.7°, this allows a momentum determination with an error of the order of 1%. The beam-energy spread is 4 MeV (FWHM). We did not use spark chambers in front of the bending magnet since the flux of particles coming straight through the pipe gives a high probability of having two sparks within the memory of a spark chamber (~ 1 μsec). Using current-division filmless chambers[8] which do not permit the detection of a double spark, we have chosen to bend the beam through a larger angle so that the uncertainties of the initial input position would be of less importance. This results in a beam which is optically worse after such a bending. A quadrupole pair focuses the pion beam onto the target T after passage through three spark chambers (SP3, SP4, SP5) giving, with redundancy, the line of flight of the pions impinging upon the target. Each of the two protons, emitted at (79 ± 10)° from the line of flight of the pions, is detected in two spark chambers (SP6, SP7, SP8, SP9), giving the spatial coordinates. It is stopped in a range assembly (R1, R2)

consisting of 50 scintillators viewed by 50 photomultipliers. The choice of this particular geometry was dictated by the fact that it corresponds, in the case of a ^{6}Li target, with protons of equal energy, to a zero recoil energy for the residual helium in the ground state. The protons also traverse two scintillation counters of 8 mm thickness (C_5 and C_6). An event is defined by a coincidence $C_1C_2C_3\bar{C}_4C_5C_6$; $\bar{C}_4$ is a counter with a hole of 4 x 4 cm, vetoing the incoming beam, and defining the active area of the target. Typically, 25,000 π^+ of 80 MeV, with a duty cycle of about 30 to 50%, hit the target per second. About 50% of the pion intensity is rejected by the veto counter defining the beam.

All the spark chambers are automatic and for each event we collect the following data:

- 18 coordinates from the 9 spark chambers SP1, 2, 3, 4, 5, 6, 7, 8, 9.
- Two pulse heights from the linear outputs of the counters C_5 and C_6. This allows a separation between protons and pions.
- The pattern of the activated counters in the range assemblies R_1 and R_2.
- A logic signal indicating whether within the memory time of the spark chambers (1 μsec) more than one particle went through. This is done simply by counting the number of particles which traversed the beam counter during the memory time.

The digitized data are stored on an IBM magnetic-tape unit, but are first processed by a PDP 8. We found that it was an essential advantage to have a computer on line. The complexity of the experiment makes it very difficult to check every parameter with sufficient regularity. The computer on line saves a great deal of machine time by giving a constant check on the parameters of the experiment.

3. EXPERIMENTAL RESULTS

The data stored on the magnetic tape are analysed by a CDC 6600. In the reaction

$$\pi^+ + A \rightarrow p + p + B$$

we calculate, among other quantities, the excitation energy of B, the three components of the recoil momentum of B and the total recoil momentum of B.

The following partial results have been obtained with a series of nuclei. We wish to emphasize that the data are not definitive. For instance, uncertainties of 2 MeV or even 4 MeV can exist for the origin of excitation energies. A careful adjustment of this point is now under way.

I. ^{6}Li

This is the target that was most studied, and that dictated our choice of geometry. For a pion of 80 MeV being absorbed by ^{6}Li and leading to a reaction where the residual ^{4}He nucleus is in its ground state, with the two protons of equal energy coplanar with the pion, this leads to a zero momentum for the recoil. If we take a model in which the absorption occurs in a pair (np) while the helium core is merely a spectator, in the impulse approximation, the momentum K of the recoiling helium is given by $K = -(k_1 + k_2 - q)$, where k_1 and k_2 are the momenta

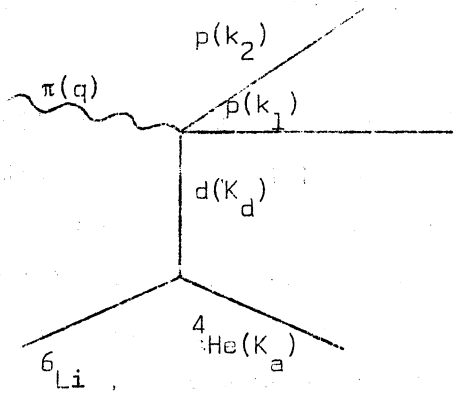

of the protons, and q is the momentum of the incident pion; $K = -K_d$, the momentum of the deuterium inside the ^{6}Li nucleus. Perturbation

theory in its simplest form gives the result that the reaction is proportional to

$$g^2(K_d^2)\ f^2(\Delta^2)$$

where g^2 is the probability of finding a deuteron of momentum K_d, and f^2 is the probability of finding, inside the cluster, two nucleons with relative momentum Δ. It is assumed that these functions are slowly varying functions when their arguments are large, while they have a maximum when the argument is zero. By choosing geometrical conditions where one of the arguments is zero, it is expected that the study of the variations of the cross-section around this geometry will give information about this function. These considerations of Jean[1] dictated our choice of geometry. However, the fact that we had to choose a large solid angle for the protons and a wide energy acceptance gives us a wide acceptance in the recoil momentum spectrum. From phase-space considerations alone, the density around zero momentum is multiplied by p^2 so that we have, in fact, no events with zero recoil energy.

Figure 2 show the spectrum of the excitation energy of the residual nucleus.

Figure 3 gives a two-dimensional plot of the excitation energy versus recoil momentum.

Figures 4a, b, c, d, e show the variation of the excitation energy for the various bands of the recoil momenta.

We see that the transition to the ground state corresponds to a peripheral process with a small momentum transfer. It is possible to calculate the momentum distribution assuming a simple cluster model, with a Hulthén-type wave function describing the relative motion of the deuteron and the helium core. Figure 5a shows the experimental momentum distribution of the ^{4}He recoils produced in the transitions to the ground state, together with a Monte-Carlo calculation of the distribution expected under our experimental conditions for such a model[3,9].

Figure 5b shows the distribution of the recoil momentum with respect to the pion beam. The distribution is symmetrical in the forward-backward directions in the laboratory showing the validity of the impulse approximation in the treatment of this problem.

We see from Fig. 4 that for recoil momenta up to 150 MeV, the second peak is mainly at 30 MeV. From 150 MeV/c onwards, the transition leads also to states close to 50 MeV. Some light has been thrown on the peak at 30 MeV by the study of ^{4}He.

II. ^{4}He

We used a liquid-helium target consisting of a vertical cylinder of 5 cm radius. Figure 6 shows the excitation energy of the residual pair of nucleons. We observe that a large fraction of the $(\pi^+,2p)$ reactions leave the np pair in a strongly interacting state. The width of the peak, 13 MeV, is larger than our experimental resolution (6 MeV), but narrower than the 30-MeV peak in the ^{6}Li. This peak can be explained within the framework of the cluster model by assuming that it is due to the absorption of the pion in the helium core. Figure 7 shows a Monte Carlo calculation of the excitation energy of the recoil from a $(\pi^+,2p)$ reaction on ^{6}Li, assuming that the absorption occurs in the helium[3]. For this calculation a naive bi-deuteron model is taken for the helium, in the absence, for the time being, of any realistic calculation fitting the helium results. Figures 4b and 4c show that the peak structure of the np recoil excitation is maintained even for the highest recoil momenta as is also observed for the 30 MeV peak in ^{6}Li. The comparison of the cross-section of the $(\pi^+,2p)$ reaction in D, He and ^{6}Li is also of importance when checking these considerations on the ^{6}Li model: we shall come back to this below, when we discuss the general question of cross-sections.

III. ^{7}Li

Figure 8 shows the excitation energy of the ^{5}He recoil. It again seems that a simple cluster model explains the two-peak structure. The second peak is distant by about 22 MeV from the ground state.

IV. ^{12}C, ^{14}N, ^{16}O

These three nuclei have been studied with targets of graphite, liquid nitrogen, and water. We group them together since Kopaleishvili et al.[4,5] have made definite predictions concerning the probability of exciting the various levels of the residual nuclei.

The calculations are made in the independent-pair model for the target nuclei. The interaction of the ejected nucleons with the residual nucleus is neglected. The interaction between the ejected nucleons is taken into account in the asymptotic approximation. The calculations are made for E_π = 40 MeV, since experimental data are available for the phases of N-N scattering at the corresponding energies. They find that the main contribution to the absorption comes from the P shell. The probability for the absorption by a pair in the S state is very small, while the probability for the absorption by a nucleon in both the S and the P shell is estimated to be at most 15%. The wave function of the nucleons of the P shell is formed from all possible products of the wave functions of the two nucleons absorbing a pion and (n-2) other nucleons. With this model they take into account all the levels of the residual nuclei with $E_K \lesssim$ 20MeV. Although they made the calculation with 40-MeV pions against 80 MeV in our case, and for a different geometry, it seemed to us interesting to fold our experimental resolution into their calculations and compare them with our results. These are the solid curves traced on Fig. 9. The cross-section scale has been adjusted arbitrarily, but we see that these authors make realistic predictions concerning the density of excitation of the different states.

Clearly, such calculations should be extended to cover the range of nuclei that we have studied, and the energy of pions we have worked with. It is striking that strong differences appear in the energy spectrum above 20 MeV, between ^{12}C and ^{14}N. The message that is contained here concerning the properties of different nuclear structures is apparently out of reach of the theory for the moment.

V. ^{9}Be, B, ^{19}F, ^{27}Al, S, Cl, ^{40}Ca, Fe and Pb

For these nuclei let us display the spectrum of the excitation energy (Fig. 10). As expected, all structures are smoothed out with increasing atomic number.

4. CROSS-SECTIONS

Since our experiment has been done in a fixed geometry subtending a small fraction of the 4π solid angle (5% for each proton), we cannot extract much information from the measurement of the cross-sections. It is known from the measurements of the angular distributions of the protons in the $(\pi^+, 2p)$ reactions in deuterium[10,11] that, in this case, the angular distribution is strongly anisotropic, of the form $1 + 3.7 \cos^2\theta$ at 80 MeV. We are sitting at the position of the minimum cross-section for deuterium. It is likely that these distributions vary for the reactions occurring on pairs sitting in different shells of the nuclei.

Thus, a correction factor varying for each energy band of the excitation energy would be necessary. The differential cross-section integrated over the solid angle and energy band of our instrument is displayed on Fig. 11. We see, for instance, that the cross-section of ^{6}Li is much higher than the sum of cross-sections of ^{2}D and ^{4}He (168 μb) against 43 μb and 53 μb for ^{2}D and ^{4}He. This shows that pairs of nucleons other than those in the deuterium and helium clusters play a role in the absorption. More interesting, perhaps, are the cross-sections for the reactions leading to the ground states of the residual nuclei. Limiting ourselves to the first 20 MeV of excitation energy, we see strong variations displaying the differences between the nuclear species. We may notice that the cross-section for the peripheral reaction on ^{6}Li is the same as the cross-section on deuterium.

5. THE $(\pi^+, 2p)$ REACTION AS A FUNCTION OF ENERGY

We have made a brief study of the reaction $(\pi^+, 2p)$ on ^{6}Li at 40 MeV, 80 MeV, 150 MeV, 200 MeV, 260 MeV. We observe a variation of the cross-section as we go through the (3/2, 3/2) resonance region, for the reactions leading to the ground state and the first excited state. Between 40 MeV and 200 MeV, the spectrum of the excitation energy varies very little. At 260 MeV, the structure is more complex, and more experiments are necessary to understand the data.

6. CONCLUSION

In conclusion, we may say that we have obtained a set of data which is raw material for which more theoretical investigation is necessary. It appears to us that since definite nuclear-structure effects appear, as shown by the comparison of our results in ^{12}C, ^{16}O, and ^{14}N with the calculations of Kopaleishvili, it will be necessary to undertake these experiments with more refined techniques giving a better resolution. The limitation in our energy resolution comes mainly from the range chambers. We have to measure two-proton spectra ranging from 40 MeV to 200 MeV. An accuracy of about 3 MeV with the range chambers is the best we have reached. The use of magnetic spectrometers and spark-chamber techniques to measure the energy of the charged particles would lead to 1-MeV resolution, as can easily be seen from the experience already acquired in this field by many groups. It would also be useful to cover a 4π angle with respect to the incoming pion.

REFERENCES

1) M. Jean, a) Proc. Int. Symposium on Direct Interactions and Nuclear Reaction Mechanism, Padua (1962); b) Nuovo Cimento Suppl. I, 2, 400 (1964).

2) G. Charpak, G. Gregoire, L. Massonnet, J. Saudinos, J. Favier, M. Gusakow and M. Jean, Physics Letters 16, 54 (1965).

3) G. Charpak, J. Favier, L. Massonnet and Č. Zupančič, Int. Conf. on Nuclear Physics, Gatlinburg, Tennessee, 12-17 Sept. 1966. CERN Preprint 66/1000/5.

4) T.I. Kopaleishvili, I.Z. Machabeli, G. Sh. Goksadze and N.B. Krupennikoua, Physics Letters 22, 181 (1966).

5) T.I. Kopaleishvili, Nucl. Physics B1, 335 (1967).

6) J. Favier, T. Bressani, G. Charpak, L. Massonnet, W.E. Meyerhof and Č. Zupančič, submitted to Physics Letters, August 1967.

7) T. Ericson, Physics Letters 2, 278 (1962).

8) G. Charpak, J. Favier and L. Massonnet, Proc. Int. Conf. on Instrumentation for High-Energy Physics Stanford, Cal., Sept. 1967, p.3.

9) Č. Zupančič, in Proc. Second Int. Conf. on High-Energy Physics and Nuclear Structure, Rehovoth (1967).

10) R. Durbin, H. Loar and J. Steinberger, Phys. Rev. 84, 581 (1951).

11) B.S. Neganov and L.B. Parfenov, Zh. Eksperim. i Teor. Fiz. 34 (1958), 767; (English transl. Soviet Physics JETP 7, 528 (1958)).

FIGURE CAPTIONS

Fig. 1 : Experimental set-up of the $(\pi^+, 2p)$ experiment at 80 MeV.

Fig. 2 : Excitation-energy distribution of the recoil X. Reaction $\pi^+ + {}^6Li \rightarrow p + p + X$.

Fig. 3 : Two-dimensional plot of the excitation energy versus recoil momentum for ^6Li.

blank	:	0, 1, 2 counts
.	:	3 to 5 counts
+	:	9 to 14 counts
x	:	above 14 counts.

Fig. 4 : Excitation energy for different bands of recoil momenta; ^6Li target

a)	1 to 51 MeV/c
b)	51 to 101 MeV/c
c)	101 to 151 MeV/c
d)	151 to 201 MeV/c
e)	201 to 251 MeV/c.

Fig. 5 : a) Recoil momentum spectrum for the reactions leading to the ground state of ^4He. Histogram 1 is the result of a Monte-Carlo calculation assuming a peripheral mechanism on the deuterium cluster in ^6Li. Histogram 2 is the distribution expected from a phase-space calculation. The points are our experimental results.

b) The same for the projection of recoil momentum along the beam axis.

Fig. 6 : Excitation energy of the recoiling np pair. Reaction $\pi^+ + {}^4He \rightarrow p + p + (np)$.

a) Excitation energy for all recoil momenta.

b) Two-dimensional plot of excitation energy versus momenta.

Fig. 7 : Excitation energy of the recoil in the reaction $\pi^+ + {}^6Li \rightarrow p + p + {}^4He$. Histogram: Result of a Monte-Carlo calculation assuming a peripheral mechanism for the absorption in the ^4He core of ^6Li.

Fig. 8 : Excitation energy of the recoil in reaction $\pi^+ + {}^7Li \rightarrow p + p + {}^5He$.

Fig. 9 : Excitation energy of the recoils with targets of ^{12}C, ^{14}N, and ^{16}O. Solid curves: predictions of Kopaleishvili et al.[4,5] with our energy resolution. Vertical scale arbitrary.

Fig. 10 : Excitation energy of the recoils with targets of ^9Be, B, ^{19}F, ^{27}Al, S, ^{40}Ca, Fe.

Fig. 11 : Differential cross-section integrated over our solid-angle and energy acceptance.

$$\sigma = \int_{\text{instrument}} \frac{d^6\sigma}{dE_1\, dE_2\, d\Omega_1\, d\Omega_2}$$

The solid angle subtended by a proton detector is 5% of 4π.

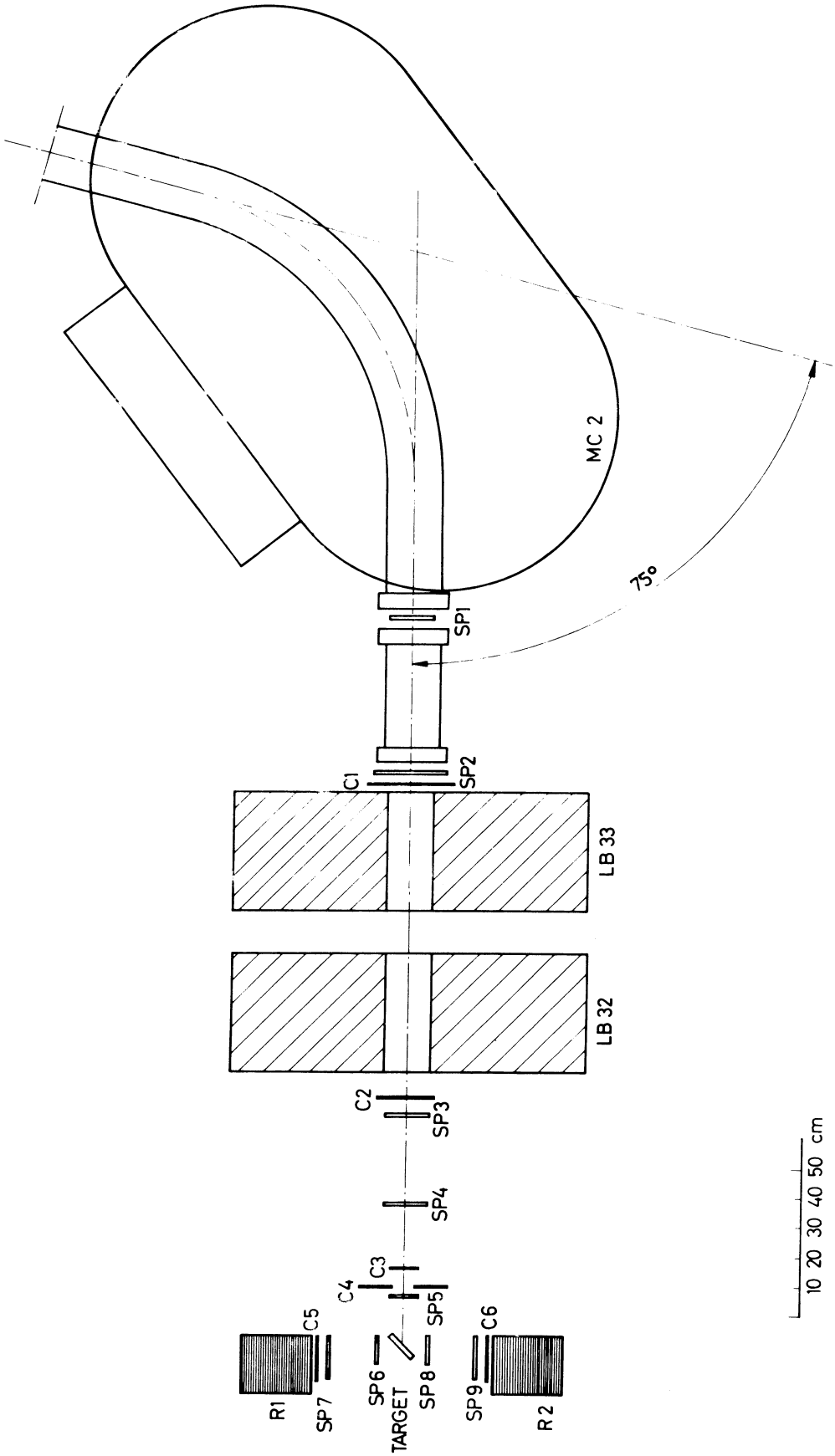

FIG. 1

DIA 31673

SIS/K 0315

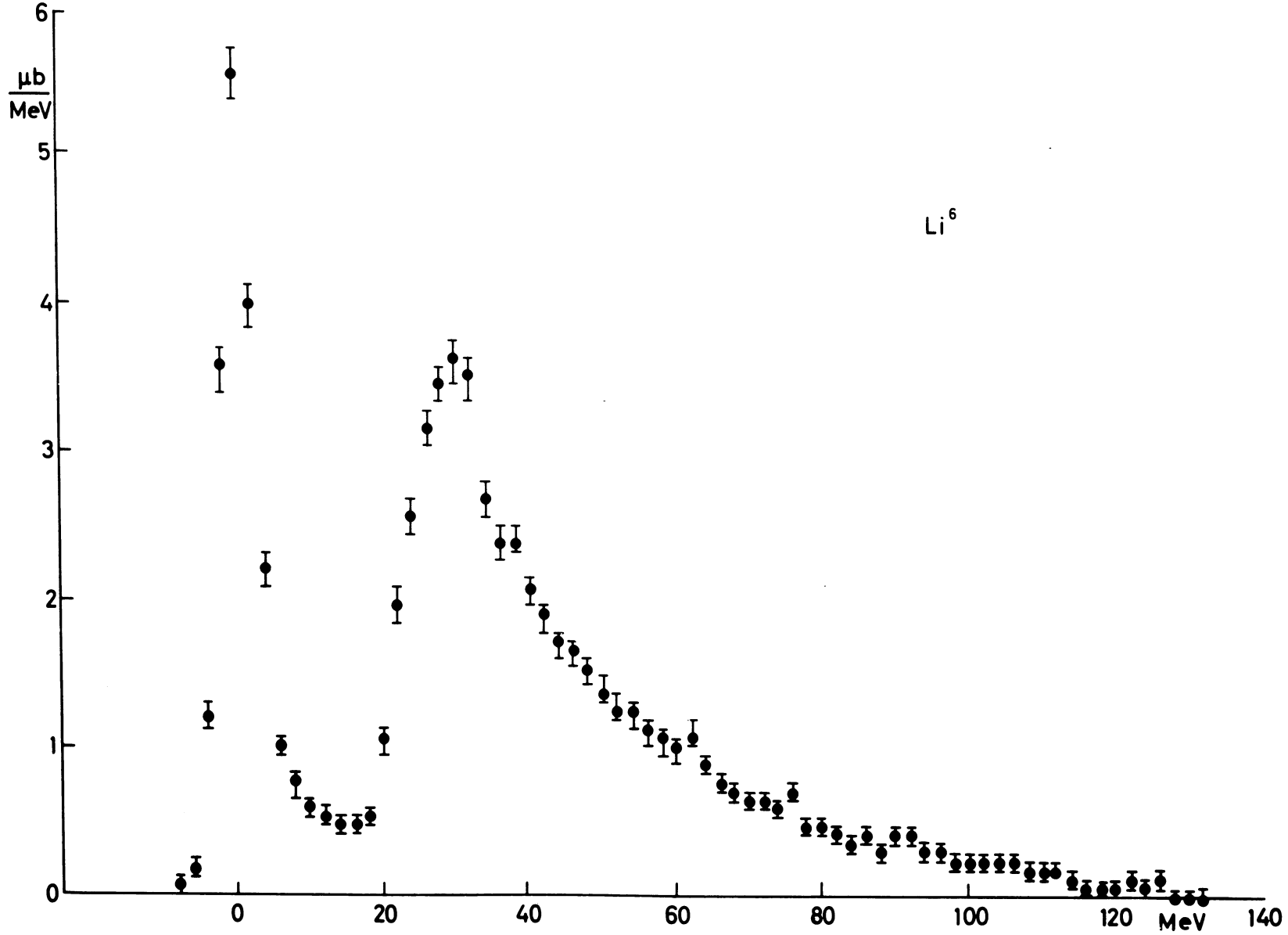

FIG. 2

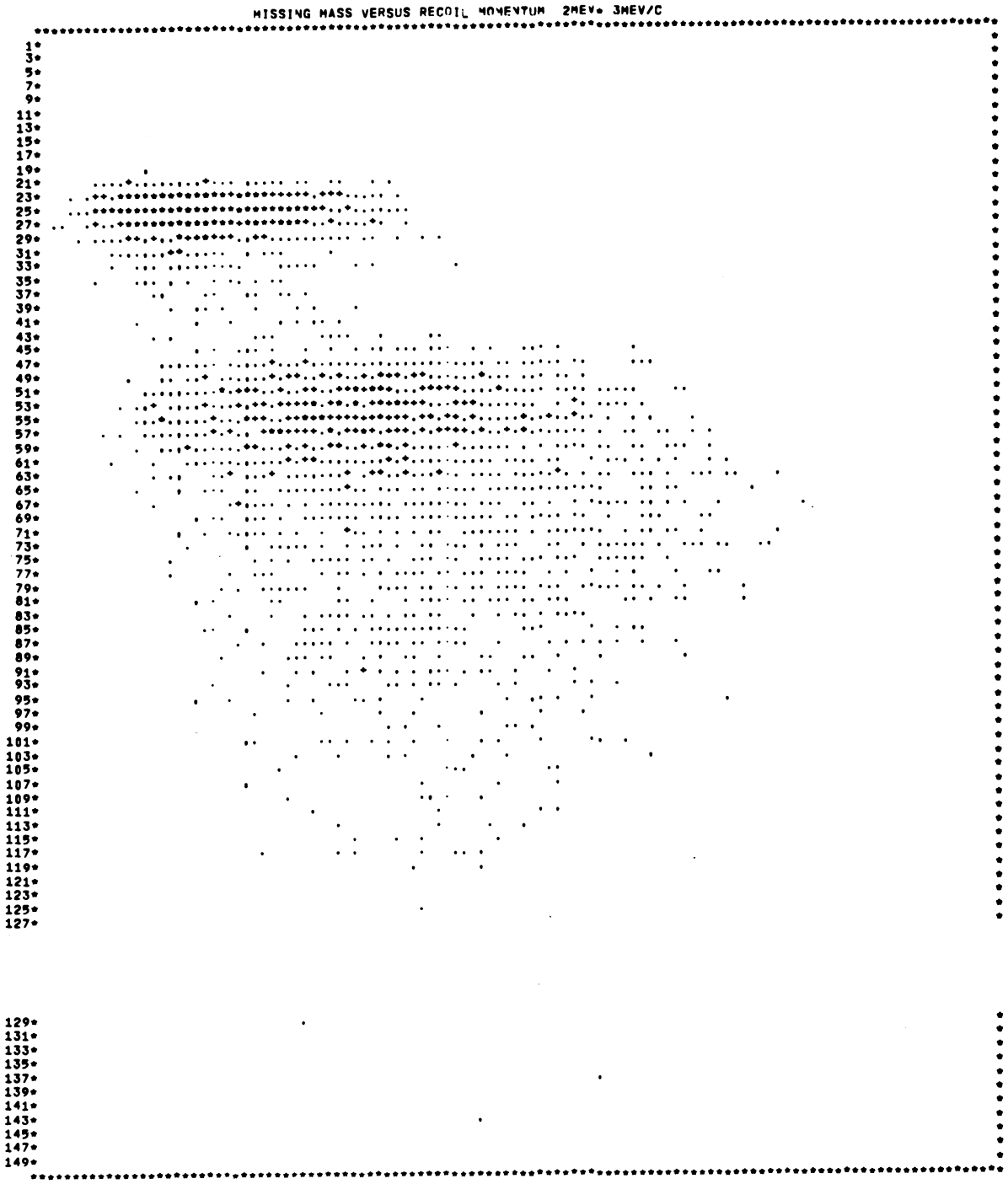

FIG. 3

DIA 31188

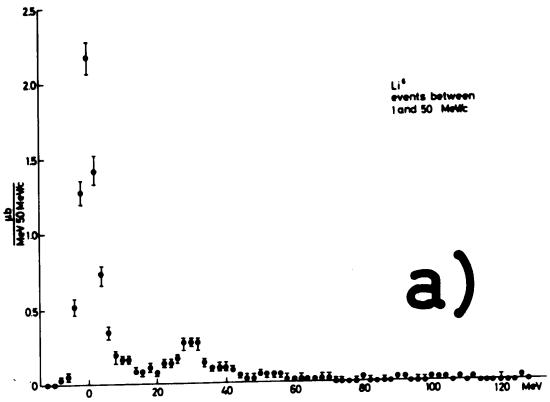

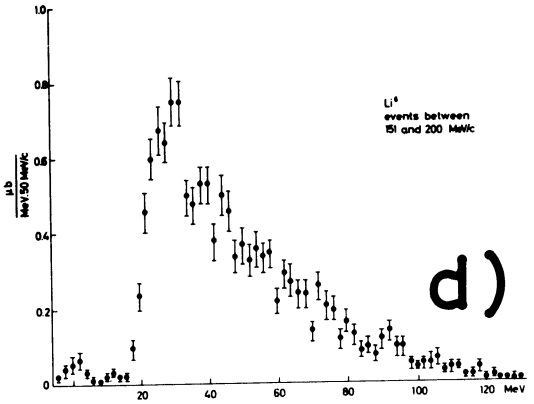

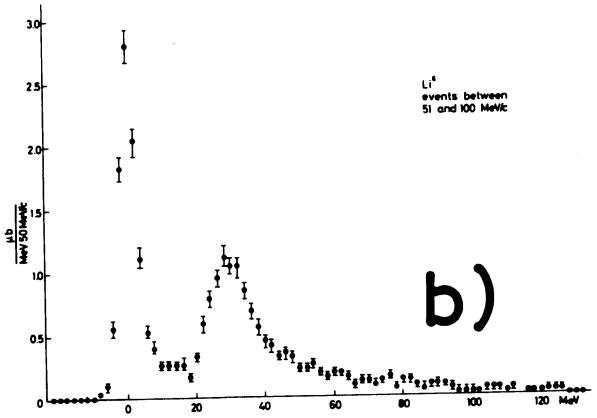

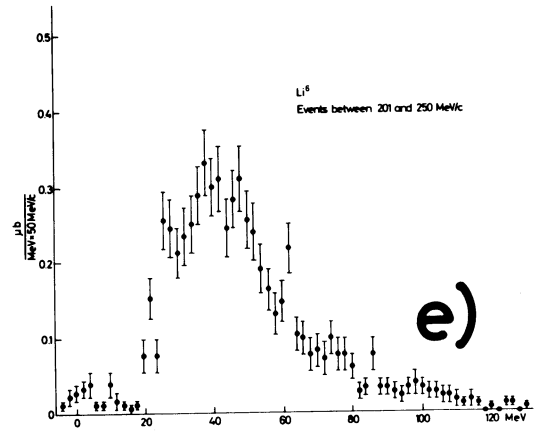

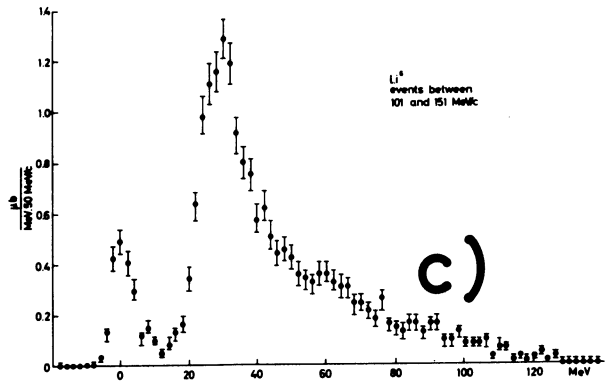

DIA 31710

FIG. 4

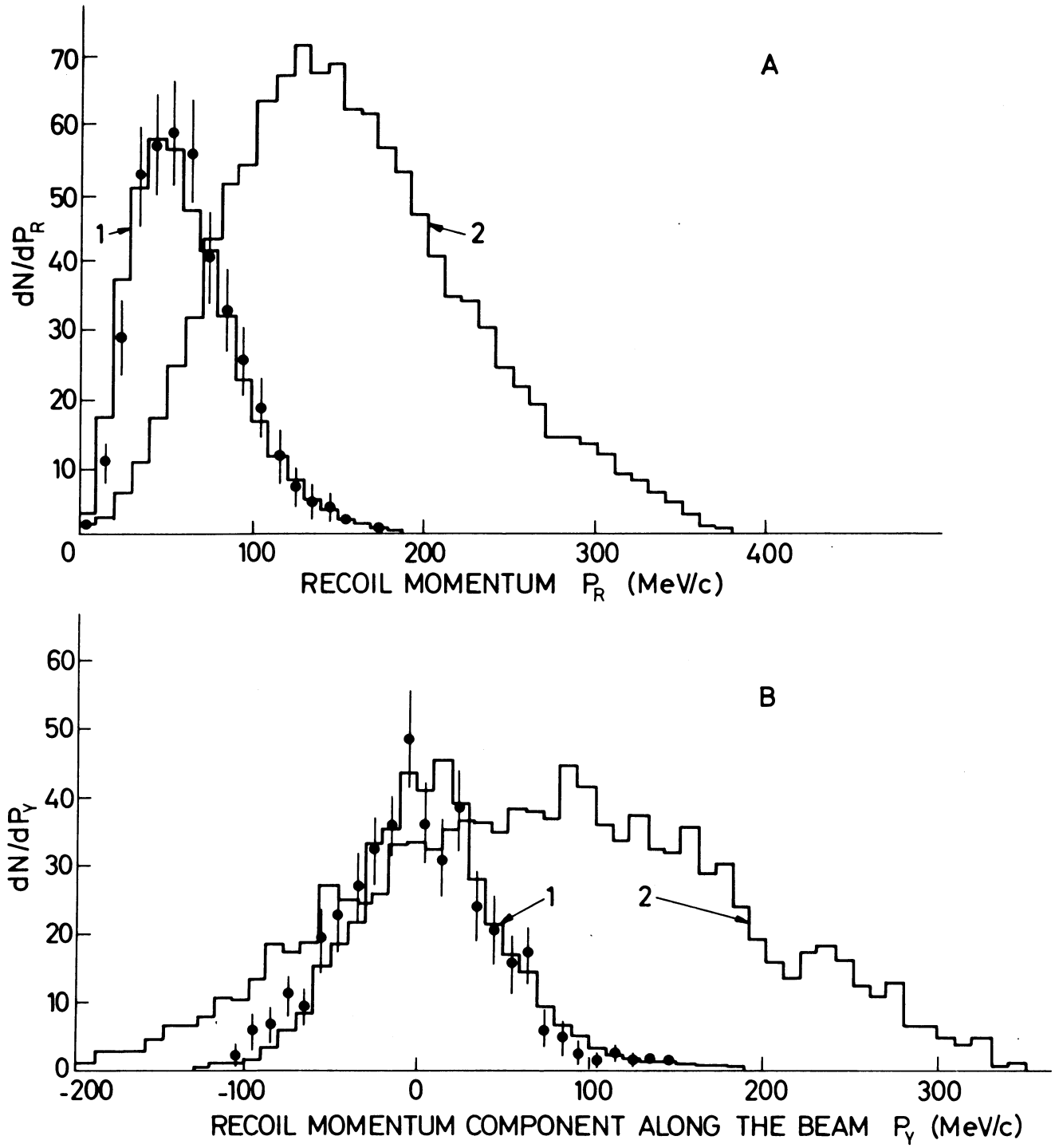
A
dN/dP_R
70
60
50
40
30
20
10
0
100
200
300
400
1
2
RECOIL MOMENTUM P_R (MeV/c)
B
dN/dP_Y
60
50
40
30
20
10
0
-200
-100
0
100
200
300
1
2
RECOIL MOMENTUM COMPONENT ALONG THE BEAM P_Y (MeV/c)

FIG. 5

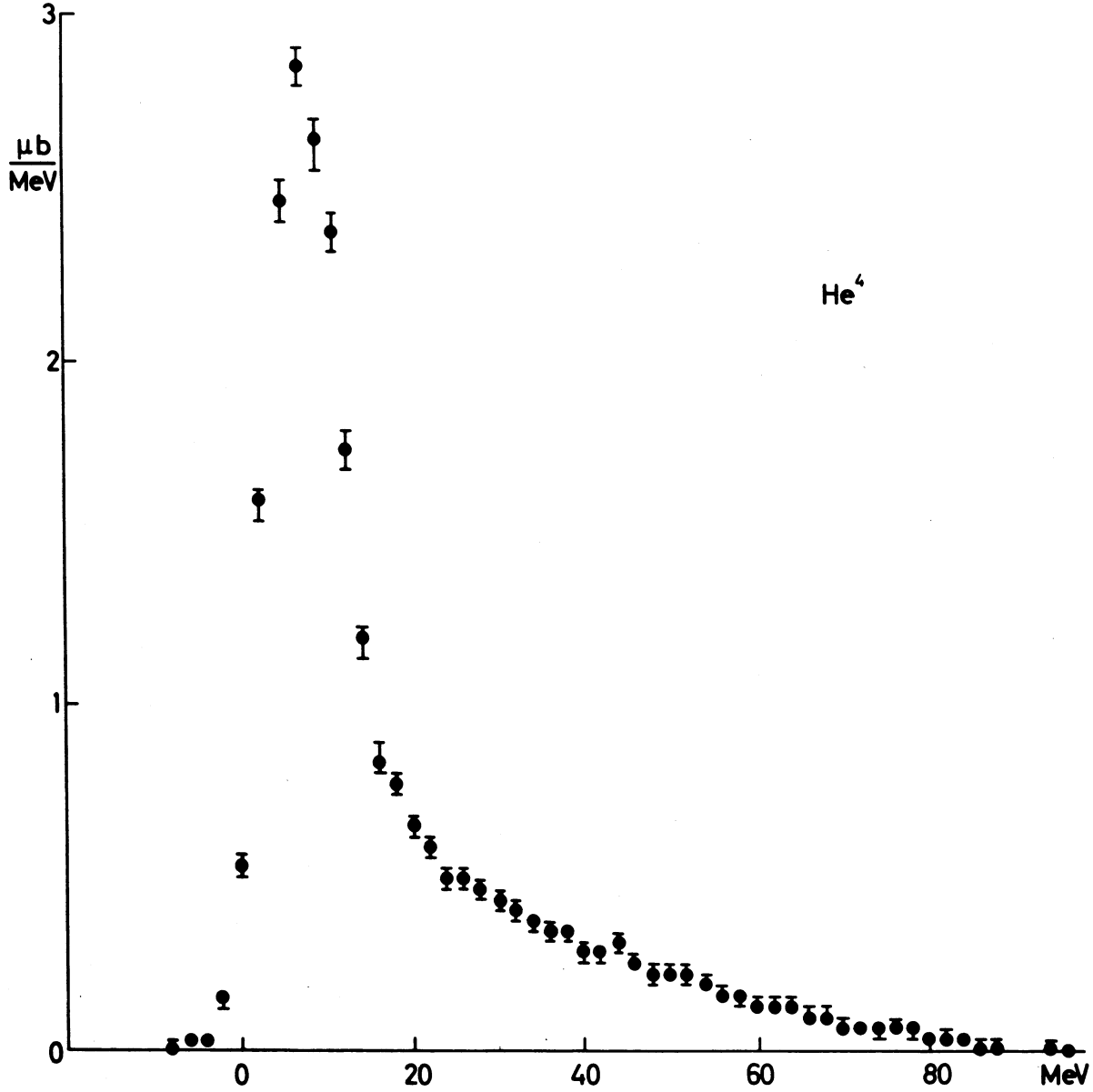

FIG. 6a

DIA 31168

FIG. 6b

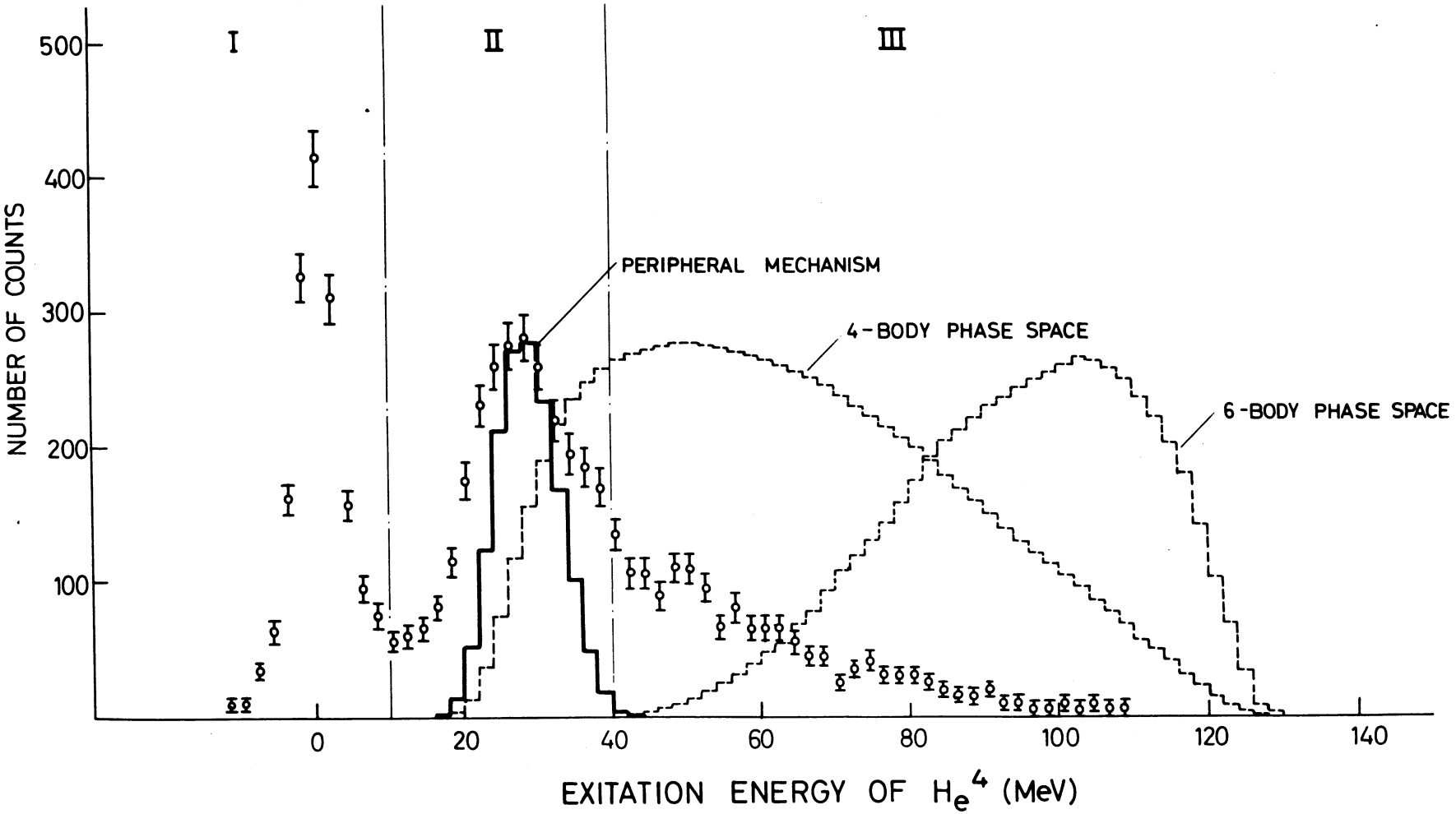

FIG. 7

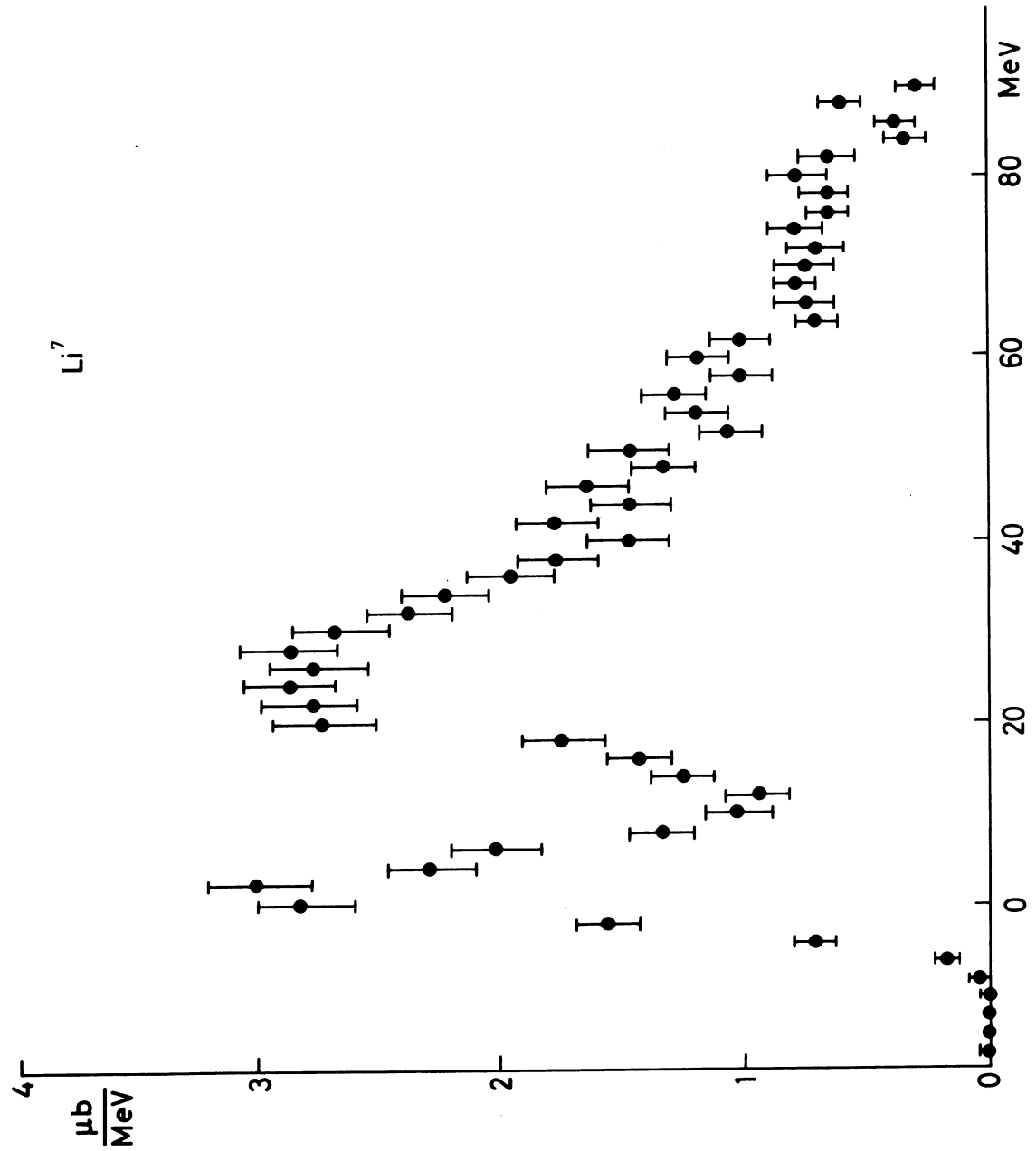

FIG. 8

DIA 31175

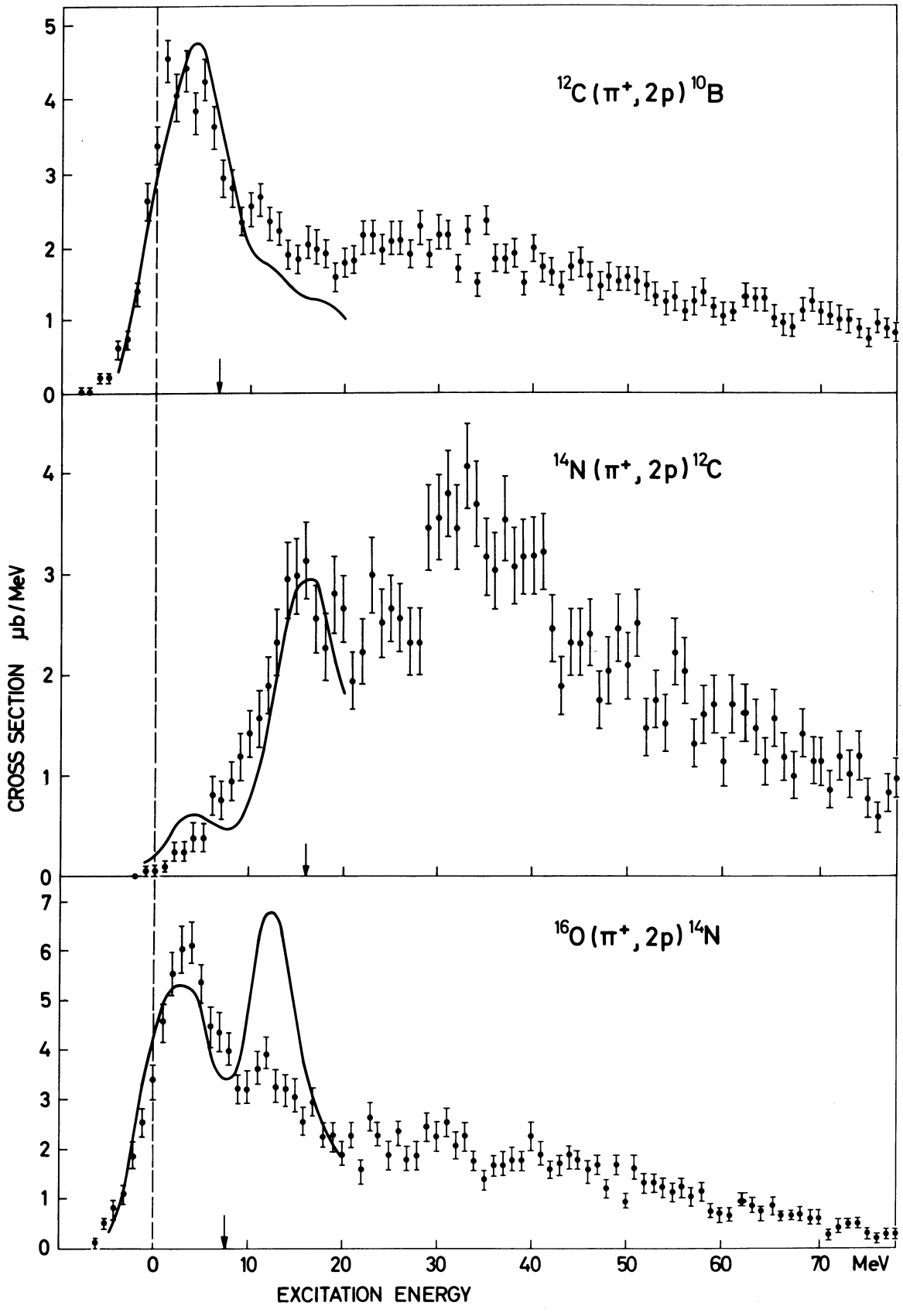

FIG. 9

DIA 30945

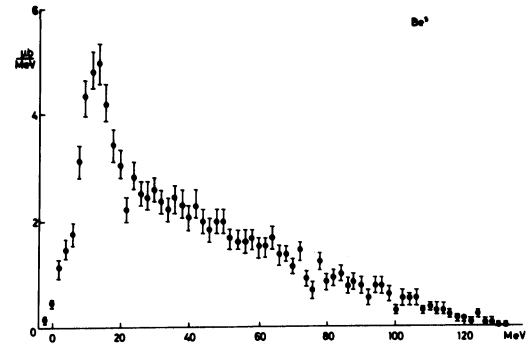

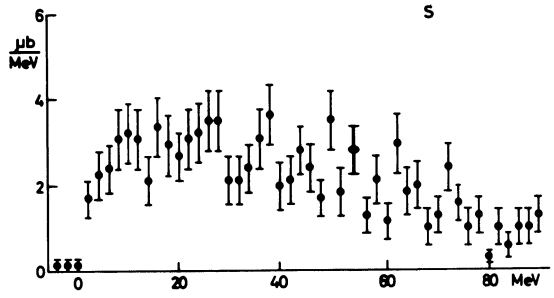

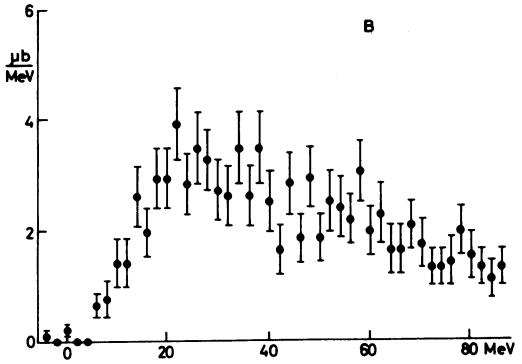

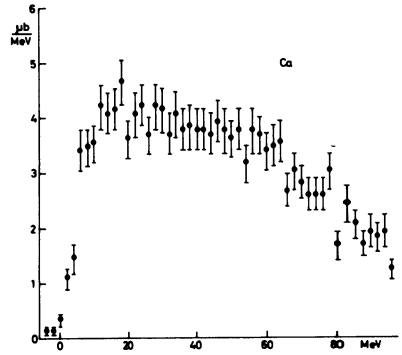

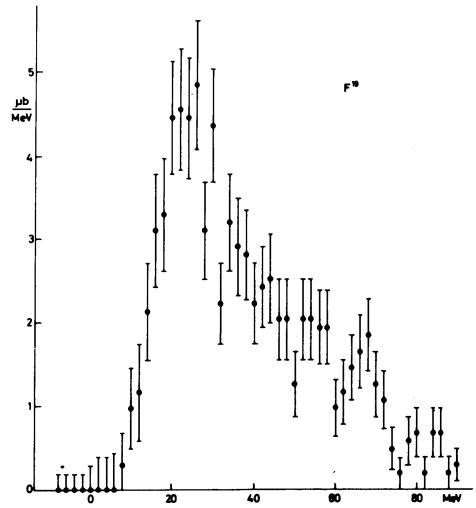

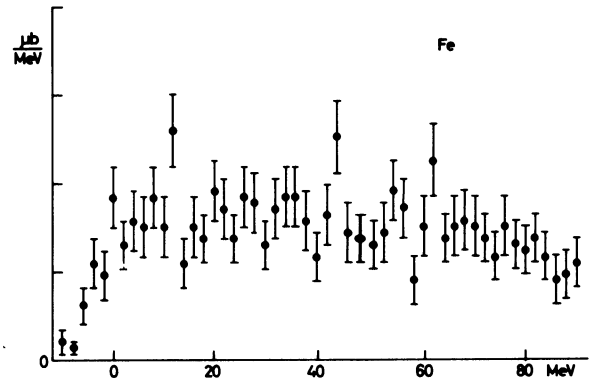

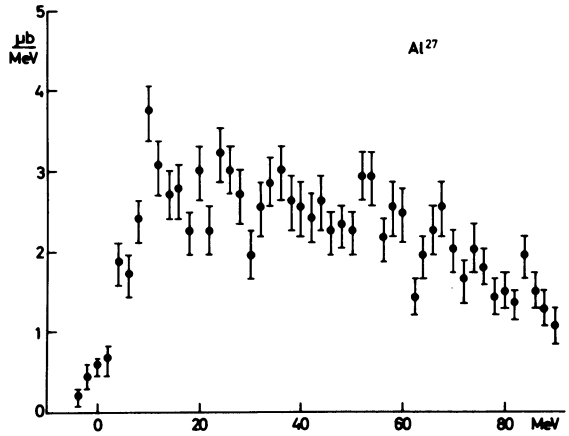

DIA 31709

FIG. 10

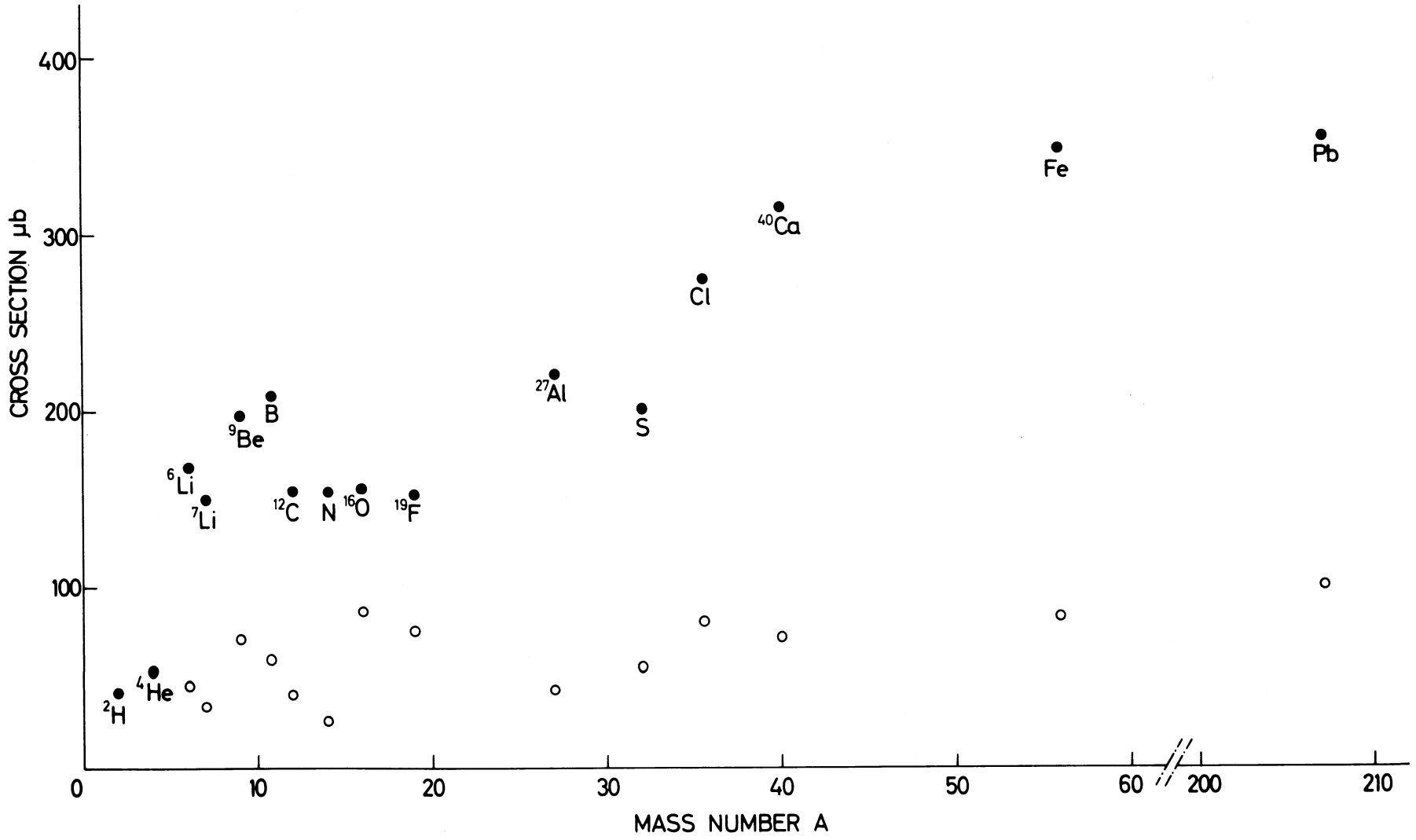
CROSS SECTION μb
400
300
200
100
0
10
20
30
40
50
60
200
210
MASS NUMBER A
^{2}H
^{4}He
^{6}Li
^{7}Li
^{9}Be
B
^{12}C
N
^{16}O
^{19}F
^{27}Al
S
Cl
^{40}Ca
Fe
Pb

FIG. 11